A novel capacitance sensor for fireside corrosion measurement

Heng Ban and Zuoping Li

Citation: Review of Scientific Instruments **80**, 115107 (2009); doi: 10.1063/1.3262500
View online: http://dx.doi.org/10.1063/1.3262500
View Table of Contents: http://aip.scitation.org/toc/rsi/80/11
Published by the American Institute of Physics

A novel capacitance sensor for fireside corrosion measurement

Heng Ban and Zuoping Li[a)]
Department of Mechanical and Aerospace Engineering, Utah State University, 4130 Old Main Hill, Logan, Utah 84341, USA

(Received 21 September 2009; accepted 17 October 2009; published online 12 November 2009)

Fireside corrosion in coal-fired power plants is a leading mechanism for boiler tube failures. Online monitoring of fireside corrosion can provide timely data to plant operators for mitigation implementation. This paper presents a novel sensor concept for measuring metal loss based on electrical capacitance. Laboratory-scale experiments demonstrated the feasibility of design, fabrication, and operation of the sensor. The fabrication of the prototype sensor involved sputtering deposition of a thin metal coating with varying thickness on a ceramic substrate. Corrosion metal loss resulted in a proportional decrease in electrical capacitance of the sensor. Laboratory experiments using a muffle furnace with an oxidation environment demonstrated that low carbon steel coatings on ceramic substrate survived cyclic temperatures over 500 °C. Measured corrosion rates of sputtered coating in air had an Arrhenius exponential dependence on temperature, with metal thickness loss ranging from 2.0 nm/h at 200 °C to 2.0 μm/h at 400 °C. Uncertainty analysis indicated that the overall measurement uncertainty was within 4%. The experimental system showed high signal-to-noise ratio, and the sensor could measure submicrometer metal thickness changes. The laboratory experiments demonstrated that the sensor concept and measurement system are capable of short term, online monitoring of metal loss, indicating the potential for the sensor to be used for fireside corrosion monitoring and other metal loss measurement. © *2009 American Institute of Physics.* [doi:10.1063/1.3262500]

I. INTRODUCTION

Fireside corrosion is the external tube metal loss (wastage) caused by chemical reactions on boiler water tubes exposed to the combustion environment in a furnace.[1,2] The leading cause of boiler tube failures is corrosion.[3,4] Corrosion leads to the thinning of the tubes and loss of more than 80% of original thickness. Corrosion has also emerged as a significant concern for current and future energy plants due to the introduction of technologies targeting emissions reduction, efficiency improvement, and fuel/oxidant flexibility. Corrosion damage can lead to catastrophic equipment failures, explosions, and forced outages, each incurring significant downtime and repair cost. Proper management of corrosion requires real-time indication of corrosion rates.[5] Knowledge of localized corrosion rates can provide the critical information needed for preventive maintenance, which can extend the overall life of these plants.[6–8] Short term, online corrosion monitoring systems for fireside corrosion, however, remain a technical challenge.

Methods for corrosion measurement or monitoring fall into three main types: downtime inspection, metal loss type, and electrochemical type.[8,9] The result of downtime inspection is of limited value for proactive corrosion management because it provides only historical data. The simplest metal loss analysis method is the weight-loss coupon; the most commonly used technique in corrosion research.[10] The coupon requires a relatively long exposure time to yield accurate results. The constraints imposed by the time of exposure naturally limit the number of data points that can be obtained from a location, and ultimately do not detect process changes quickly.

Metal loss type sensors, however, can be combined with electrical resistance measurement to provide an online monitoring capability. Because the electrical resistance of a current path increases as its cross-sectional area is reduced, metal loss can be detected by an electrical resistance-measuring instrument.[10–12] An electrical resistance sensor is often comprised of a sensing element that is basically a wire, strip or tube made of the alloy of concern, which is used to conduct an electric signal. When the sensor element is exposed to a corrosive environment, the cross-sectional area of the element decreases, hence the resistance of the sensing element increases. Therefore, the rate of metal loss can be recorded as a function of time. Unlike electrochemical methods, resistance sensors continue to function in the presence of nonconductive scales and are valuable tools for detecting underdeposit corrosion. Resistance sensors are simple, relatively inexpensive, and are often the mainstay of a monitoring program in low-temperature applications, especially in the petroleum industry. In high-temperature combustion applications, however, resistance sensors are not commonly used because of significant thermal and thermoelectric noises.

Electrochemical techniques measure the corrosivity of an environment independent of actual material loss. Linear polarization resistance is the most widely used technique of this type.[13] It measures the dc current through the metal/fluid

[a)]Present Address: Mechanical and Aerospace Engineering, University of Virginia, 1011 Linden Avenue, Charlottesville, VA 22902, USA.

interface when the electrodes are polarized by a small electrical potential. As this current is related to the corrosion current, that in turn, is directly proportional to the corrosion rate, the method provides an instantaneous measurement of corrosion rate. It has advantages over metal loss methods but is limited in the scope of its application due to the requirement that the fluid must be conductive, which, in practice, usually limits it to aqueous solutions. There are also other electrochemical techniques include potentiostatic, galvanostatic, potentiodynamic, galvanodynamic, and ac impedance spectroscopy. None of these approaches have been developed for fireside applications as continuous monitors due to a variety of technical issues.

Electrochemical noise (ECN) is a passive electrochemical technique that requires no polarizing current but measures the naturally occurring electrochemical potential and current disturbances that result from corrosion.[14–20] The method uses current variations between two nominally similar working electrodes, whereas potential noise is based on alterations between a working electrode and a stable, reference electrode. ECN is capable of returning accurate indications of general corrosion, pitting, and stress cracking when it is properly applied but requires both expertise and complex data processing to be effective. Because ECN requires monitoring of very small signal fluctuations, this approach is also susceptible to extraneous sources of signal noise in the plant environment.

In summary, downtime inspection and metal loss coupons remain the primary techniques used to assess the fireside corrosion in power plants. Technologies with online monitoring potential are still being developed for plant applications. Most efforts have focused on adapting existing technologies from low temperature applications to fireside measurement. These technologies, however, are in their infancy and many have been found to be significantly affected by interferences inherent to the harsh combustion condition and power plant environment.

This paper reports the development effort of a novel sensor concept based on electrical capacitance for corrosion monitoring and a laboratory measurement system for short term, online fireside corrosion monitoring. The main objective of the research was to perform laboratory experiments to examine the feasibility of the concept and sensor design. Metal loss experiments were conducted using the prototype sensor in a muffle furnace to investigate sensor sensitivity, detection limit, and uncertainty range.

II. SENSOR PRINCIPLE AND METHODS

A. Sensor principle

The principle of the novel sensor is to convert the thickness measurement (i.e., the loss of a thin layer of metal due to corrosion), to an area measurement. The design of the sensor is similar to an electrical capacitor and the signal is measured by electrical capacitance (EC). An EC sensor consists of a thin ceramic substrate with metal coatings on both sides. The frontside coating that is exposed to the combustion environment has a linear thickness variation. A backside coating of noncorroding material is used to form a plate capacitor, as illustrated in Fig. 1.

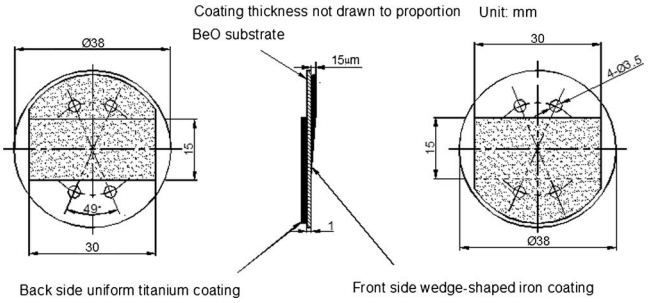

FIG. 1. Schematic drawings of the sensor used in this study.

The sensor capacitance is a function of the overlapping area of metal coatings, substrate thickness, and dielectric constant. When there is metal loss on the frontside coating, the corresponding area of the frontside coating will become smaller. Therefore, there will be a decrease in capacitance caused by the decrease in overlapping area. The corrosion rate can be measured by the decrease in electrical capacitance over the time. Because the frontside coating exposed to corrosion has a small slope, this design equivalently magnifies a small change in thickness to a much larger change in area as illustrated in Fig. 1, which is easier to measure by electrical capacitance. For instance, the thickness of the coating varies continuously from 0 to 40 μm over a length of 4 cm. Such a design converts the thickness change of 1 μm to a length change of 1 mm, and 2.5% capacitance change. The corresponding change in capacitance caused by the change in thickness can be determined theoretically based on the sensor coating geometry and the dielectric constant of the ceramic plate and calibrated experimentally on the same sensor.

The corrosion rate R in this study is defined as rate of coating thickness reduction

$$R = \delta_c/\Delta t, \tag{1}$$

where δ_χ is the coating thickness reduction perpendicular to the surface, and Δt is the exposure time. The corrosion rate can be expressed as the capacitance change by

$$R = \left(\frac{\Delta C}{C}\right)\frac{h}{\Delta t}, \tag{2}$$

where h is the maximum thickness of the initial coating. It is apparent that the percent decrease in capacitance represents the percent reduction in the coating thickness. The corrosion rate can be determined based on the percent change of the initial coating thickness as a function of time.

B. Substrate material selection

The physical and chemical properties of the sensor substrate material are important factors affecting the sensor design and its performance. Since the sensor is to operate as an electrical capacitor for corrosion monitoring in high temperature and corrosive combustion environments, it requires that the substrate material has properties of high thermal conduc-

TABLE I. Properties for BeO, AlN, and alumina (99.6% Al_2O_3).

Property	BeO	AlN	99.6% Al_2O_3
Electrical			
Dielectric constant at 1 MHz	6.7	9.1	9.8
Dielectric loss at 1 MHz	0.0002	0.0004	0.0001
Dielectric Strength (kV/mm)	>9.5	>15	35
Electrical resistivity (Ω cm)	$>10^{14}$	$>10^{12}$	$>10^{14}$
Mechanical			
Density (g/cm^3)	2.88	3.27	3.75
Young's modulus (GPa)	340	350	390
Thermal Properties			
CTE($\times 10^{-6}$/°C) (25–400 °C)	6.7	4.7	6.9
Thermal conductivity (W/Mk)	290	200	30

tivity, low thermal expansion, good electrical insulation, corrosion resistance, and stability in high temperature environments.

The substrate of the sensor should be a ceramic plate with high thermal conductivity in order to minimize temperature nonuniformity on the sensor surface. Because the dielectric constant is a function of temperature, a uniform temperature can minimize the uncertainty originated from the variation in dielectric constant. There are a few ceramic materials that have high thermal conductivity including beryllium oxide (BeO), aluminum nitride (AlN) and alumina (Al_2O_3). The comparisons of relevant properties of these materials, collected from published information, are provided in Table I.

BeO is a ceramic material that combines excellent electrical insulation properties with high thermal conductivity and resistance to corrosion. This unique combination of properties in conjunction with good mechanical strength and thermal shock resistance make BeO one of the best substrate materials for the sensor in this study. BeO powders, however, are toxic when inhaled or ingested, which requires fabrication at certified locations, significantly impacting end-user costs. It was, however, selected for this laboratory study, even though other ceramic materials (e.g., alumina) can also be used as the substrate for the capacitance sensors at a lower cost.

Aluminum oxide or alumina was the second choice for the sensor substrate although their thermal conductivity is not as high as BeO. The high volume resistivity, chemical stability at high temperature environments, high dielectric constant coupled with low dielectric loss, and excellent electrical insulation lead to its wide applications in electronics as substrates. Its cost is much lower than BeO, which makes it an attractive choice if the sensor is to be developed for industrial applications. Aluminum nitride is another ceramic material with high thermal conductivity and low coefficient of thermal expansion. The main drawback of AlN is its potential reactivity with water vapor in moist, high temperature environments making it inappropriate for combustion environments. This novel corrosion sensor, however, can potentially be used for low temperature or aqueous applications besides fireside environment, where AlN can be a good candidate.

Because the dielectric constant of sensor substrate is usually a function of temperature and there are temperature fluctuations during the measurement, it is important to obtain the relationship between the dielectric constant and temperature because the measured capacitance is temperature dependent through the dielectric constant of the ceramic substrate. A change in sensor capacitance could be caused by two sources: corrosion of the frontside coating or sensor temperature change. To eliminate the capacitance change from the sensor temperature variations and obtain the corrosion rate, a temperature compensation technique is used to process the database on measured sensor temperature and the relationship between the temperature and dielectric constant. The compensation procedure can remove the influence of temperature variations in capacitance measurement.

C. Sensor design and fabrication

Fabrication of the wedge-shaped coating on the sensor substrate is the key to the sensor concept. Figure 1 shows the schematic design of the sensor used in this study. The sensor has a wedge-shaped, low carbon steel coating on the frontside, and a uniform, corrosion-resistant titanium coating on the backside. The thickness of frontside coating varies linearly from 0 to 1.5 μm over a length of 15 mm. With the width of the coating at 30 mm, the sensor has total overlapping area of 450 mm^2.

The fabrication of the sensor used dc magnetron sputtering deposition technology to coat both sides of ceramic substrate. A Denton DVI-SJ-24 multicathode dc/rf magnetron sputtering deposition system was used to deposit the steel coating on the corrosion side and titanium coating on other side of the substrate. The shape of the coating area was obtained by specially designed masks on the substrate. To achieve linear thickness change of the frontside coating, a slow moving shutter was designed and incorporated into the sputtering chamber. The shutter gradually adjusted the exposed area of substrate for sputtering at a steady speed. The edge with most exposure time had the maximum coating thickness, while the edge with the least exposure time had the minimum thickness. The backside coating had same sputtering exposure time and a uniform thickness. The substrate was mounted on a rotating stage during the sputtering deposition in order to achieve uniform deposition. Low carbon steel 1010 was used as the target material to create wedge-shaped coatings. For the backside coating, titanium was used to provide better resistance to oxidation.

D. Temperature compensation and corrosion rate

Temperature variation in the sensor element can produce capacitance fluctuations because the dielectric constant of the substrate is a function of temperature. It was found experimentally that the dielectric constant of the BeO substrate increased with temperature. In order to eliminate interference from temperature variations, the sensor capacitance has to be evaluated and compared at a constant or nominal temperature. The fireside sensor is likely air cooled to maintain a temperature close to the boiler tube surface temperature. Small temperature fluctuation is expected to exist on the sensor under air cooling, for instance, ±2 °C. Therefore, a pro-

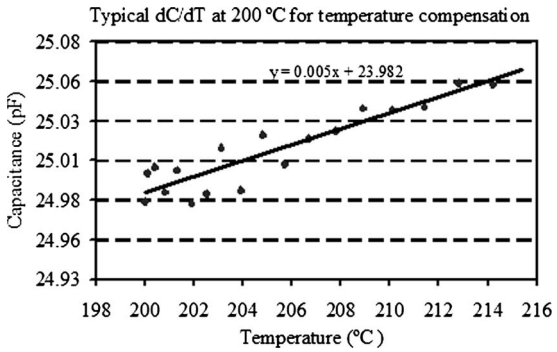

FIG. 2. A plot of dC/dT measured from small temperature fluctuations around 200 °C.

cedure for temperature compensation was developed to remove the capacitance fluctuation caused by temperature fluctuations. The compensated capacitance of the sensor element $C(T,t)$ under nominal temperature T at transient time t is calculated by Eq. (3)

$$C(T,t) = C(T',t) - \frac{dC}{dT}(T' - T), \tag{3}$$

where $C(T',t)$ is the measured sensor capacitance at temperature T' and time t, and $(T'-T)$ is the temperature difference or fluctuation from the nominal temperature T. The value of dC/dT can be determined from the temperature dependent dielectric constant of the ceramic material.

A more accurate method is to obtain dC/dT value experimentally from the actual sensor element around the temperature of interest. The recorded data include sensor capacitance and sensor temperature. The small variations in temperature around its set point, together with change in capacitance for a short period can be plotted to acquire the dC/dT value, which can be approximated as a constant. Within the short period, the actual corrosion is negligible for the sensor. The resulting capacitance-temperature relationship can be used to compensate for the temperature fluctuations in capacitance calculation. Figure 2 shows the data of temperature dependent capacitance recorded around 200 °C, and the result of dC/dT was used for temperature compensation of the measured capacitance.

Using the method, dC/dT values can be obtained at other temperature ranges and at any moment of the corrosion measurement. It allows frequent calibration of the capacitance-temperature relationship during the experiment. After temperature compensation, the true capacitance decrease ΔC of the sensor element caused by corrosion during exposure time $(t-t_0)$ can be found using Eq. (4)

$$\Delta C = C(T,t) - C(T,t_0). \tag{4}$$

Thus, the corrosion rate R at a nominal temperature T can be determined by Eq. (5)

$$R = \frac{\Delta C}{C}\frac{h}{(t-t_0)}. \tag{5}$$

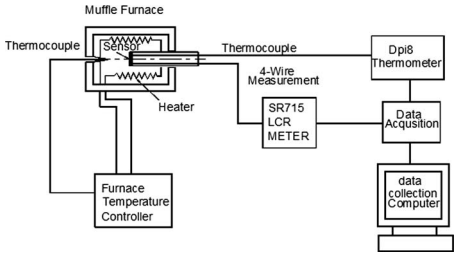

FIG. 3. Schematic diagram of the measurement system.

E. Experimental setup

An experimental system consisting of a muffle furnace, sensor element, air-cooled probe, capacitance meter, and data acquisition system was set up in the laboratory, as shown in Fig. 3. The furnace was set at a high temperature with temperature control. The sensor was placed in the muffle furnace by an air-cooled probe, which maintains the sensor element temperature. A thermocouple was installed on the sensor element to record the temperature of the sensor. The data acquisition system was programmed to perform automatic data collection by a computer to obtain the data from the SR715 *LCR* meter and OMEGA Dpi8 thermometer on a real time basis. The four-wire measurement technique was used to measure the capacitance of the sensor, with one pair of leads to supply test current to the sensor and a separate pair of leads to measure the voltage. This technique eliminates the impedance of the leads in the probe and improves measurement accuracy.

III. RESULTS AND DISCUSSIONS

A. Dielectric constant measurement

The purpose of this measurement was to determine the quantitative influence of temperature on the dielectric constant of BeO because the correlation between the dielectric constant of BeO substrate and temperature is not available in the literature at the ac frequency range of this measurement. Experiments were conducted using a BeO substrate with coatings on both sides, similar to the sensor element, and varying the furnace temperature from room temperature to over 400 °C. Results in Fig. 4 demonstrate that the dielectric constant of BeO is highly temperature dependent, and increases from 6.6 at 150 °C to 7.9 at 450 °C. The dielectric constant and temperature correlation were used in the sensor

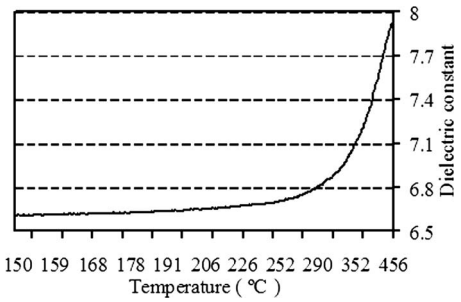

FIG. 4. Dielectric constant change of BeO as a function of temperature at 10 kHz.

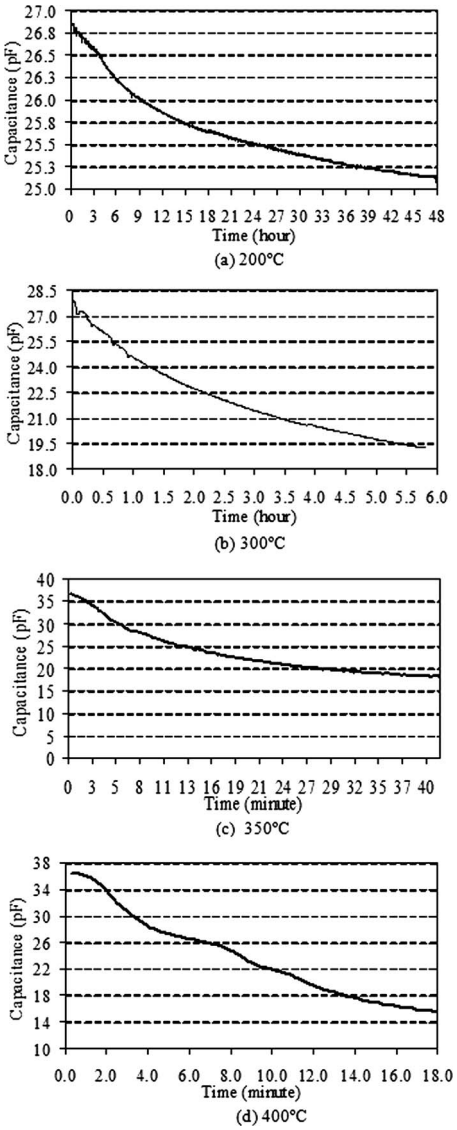

FIG. 5. Sensor capacitance change during corrosion tests at different temperatures.

design, in the selection of the measurement instrument, and in the process of evaluating uncertainties introduced by the temperature fluctuation.

B. Corrosion measurement results

Experiments were also conducted to verify that sensors can survive temperature cycles up to over 500 °C. Optical microscopy analysis of the temperature-cycled sensors indicated that the coatings survived high temperature tests without any peeling or detachment from the substrate. Laboratory corrosion experiments were performed at temperatures of 200, 300, 350, and 400 °C. To validate corrosion rates obtained by capacitance, all corroded sensors were subjected to postexposure analysis using scanning electron microscope (SEM) and a profilometer for actual corrosion. The range of temperature fluctuation during experiments was controlled within ±2 °C around the nominal temperature and temperature compensation was applied to process experimental data. The processed data in Figs. 5(a)–5(d) were obtained by using ten–point moving average. Because the reduction in coating thickness and capacitance decrease are proportional, which follows Eq. (5), the vertical axis in these figures can be considered relative coating thickness. Figures 5(a)–5(d) show that the capacitance of the sensors decreased steadily during the period of corrosion under all temperature conditions.

The results in Figs. 5(a) and 5(b) were obtained using the same sensor element. The sensor was first corroded at 200 °C for 48 h and then the temperature was increased to 300 °C for further corrosion for an additional 6 h. After cooling, the capacitance of the sensor was decreased by 50.4% from the initial capacitance value before corrosion at room temperature. Meanwhile, using the calculated average corrosion rates and integrating over exposure time, the total percentage of capacitance reduction in the sensor is 46.2%. The difference of 3.4% between the values calculated from different methods could be caused by various factors including measurement uncertainty.

Figures 5(c) and 5(d) show the results under 350 and 400 °C from two separate sensors, respectively. The corrosion experiments were carried out at 350 °C for about 45 min and 400 °C for 30 min. The total percentages of capacitance decrease were 79.1% at 350 °C and 67% at 400 °C by measuring the difference before and after the test at the room temperature. Using the calculated corrosion rates, the same values derived from the integral method were 70.9% for 350 °C and 65% for 400 °C, respectively.

The results indicate that the system can measure capacitance change of the sensor to about 1% of the initial capacitance. In fact, capacitance data fluctuation shown in Fig. 2 was only about 0.05 pF, much less than 1% of the measurement range. Because the total capacitance was about 30 pF for this experimental design, and it was corresponding to the maximum coating thickness of 1.5 μm, the detection limit for thickness change for the coating was 15 nm. As a result, an accurate metal loss measurement was achieved in periods as short as a few hours under 200–400 °C conditions.

The sensitivity of the capacitance method depends on the sensitivity of the fabricated sensors and the precision of instruments used. The sensitivity of the sensors was determined by the slope of the wedge-shaped coating, its initial coating thickness, sensor geometry such as the overlapping area, and the dielectric constant of substrate material. Further understanding the relationship of these parameters and sensitivity will be useful to optimize the sensor design and the measurement system.

The experiments clearly demonstrated the feasibility of the sensor concept. In real fireside corrosion cases, typical range of the normal corrosion is about 1 μm per day for water walls in a pulverized coal, wall-fired boiler. Using this type of sensor of maximum thickness, for instance, 15 μm, it is feasible to determine carbon steel loss rate in a day or two, while the sensor can last two weeks in the furnace at typical water wall temperatures about 300–400 °C. Higher corrosion rates will be much easier to detect. As a contrast, typical corrosion coupon tests take months to return corrosion rates. This novel capacitance fireside corrosion sensor can provide much quicker detection of corrosion condition if the operation condition of the furnace is changed.

The average corrosion rates of experiments are summa-

TABLE II. Average corrosion rates with uncertainty at different test temperatures.

Sensors	Corrosion exposure time (h)	Temperature (°C)	Corrosion rate with uncertainty (nm/h)
1	48	200	1.98 ± 0.07
2	6	300	56 ± 2.0
3	0.75	350	1520 ± 38
4	0.5	400	1970 ± 62

rized in Table II. The temperature dependence of steel corrosion rate is evident from the data. Arrhenius form of rate equation was used to approximate the temperature effect. The average volume corrosion rate (i.e., iron oxidation reaction in air) is a function of the exposed surface area (4.5×10^{-4}, in m^2), oxygen concentration (at different experimental temperatures, in mol/m^3), a pre-exponential factor A, and an exponential term with activation energy E, and temperature T. The corrosion rate in terms of thickness reduction (m/s) can be written as

$$R = \mathrm{O}_2 \ \text{Concentration} \times A \times e^{-\frac{E}{R_u T}}, \tag{6}$$

where R_u is the universal gas constant, 8.314 J/mol K. The average corrosion rate data were plotted in Fig. 6 with the logarithmic dimensionless thickness reduction rate, $\ln[R/(\mathrm{O}_2 \ \text{Concentration} \times A)]$ as a function of $1/T$. The data had a reasonably good fit, indicating the temperature dependence of iron oxidation generally follows the Arrhenius rate. The resulting activation energy is 100 kJ/mol, and the pre-exponential factor is 0.0135 $m^4/(\text{mol}\cdot\text{s})$. The average corrosion rate in thickness reduction can be estimated using the activation energy and pre-exponential factor for the coating fabricated in this study.

Because sputtered low carbon steel is a dense material with a different microstructure from the original target material, its corrosion rate is expected to be different from the original material. In addition, because the sputtered coating has a fresh surface, the initial corrosion rate is expected to be high due to the lack of an oxidized layer. The experimental data in Fig. 5 show that the capacitance of the sensors decreased quickly once the corrosion experiments started. As a layer of oxide scale built up, the corrosion rate decreased with exposure time. If such a sensor is used to monitor fireside corrosion, the measured corrosion rate is likely to reflect the general corrosion characteristics. It will provide semiquantitative corrosion information comparatively. The measured rate using such a sensor element, however, has to be calibrated to provide a quantitative measure of corrosion rate of the low carbon steel of boiler water walls. Resistance sensors with sputtered coating are commercially available for low temperature applications. Calibrations and correlations for such applications are well established. For high temperature applications, calibrations and correlations can be established in a similar way once this type of sensors is widely used.

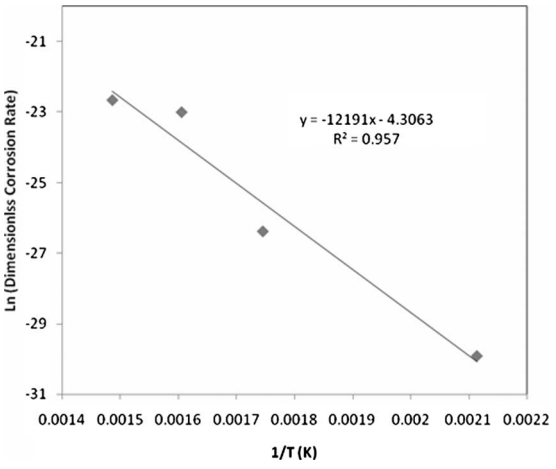

FIG. 6. Arrhenius plot of measured corrosion data.

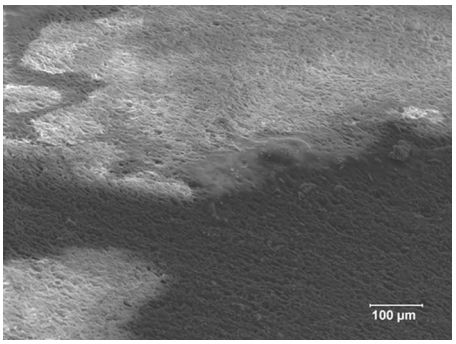

FIG. 7. SEM photomicrograph of coating boundary of a corroded sensor.

C. Profilometer, optical microscope, and SEM analysis

Analysis of the new and corroded sensor elements included optical and SEM morphological examinations and thickness measurement using a profilometer. The coating boundary and the transition area shown in Fig. 7 illustrate the areas of thinnest coating of the substrate after corrosion. The surface was lightly brushed to remove the loose layer of rust. The thin coating layer appears to follow the surface roughness features of the substrate; however, the capacitance result did not show any effect of roughness in terms of the sensor function to determine corrosion rate. The surface roughness would not be an issue if the coating was thicker for industrial applications. A surface stylus profilometer (Alpha Step 500) was used to measure the coating thickness of new sensor elements and provided quantitative verification of the coating thickness and slope. It was not able, however, to determine the coating thickness change after corrosion because the process requires a special sensor design in addition to the uncertainties caused by different surface cleaning processes.

D. Uncertainty estimation

Uncertainty analysis of the corrosion measurement was carried out to quantify the uncertainty of the measurement system. The corrosion rate in this research is a multivariable indirect measurement, and the measurement uncertainty from each variable propagates to the final result or overall uncertainty. Therefore, the corrosion rates with uncertainty for the experimental results under different temperatures were calculated based on experimental or estimated precision and

bias uncertainties of individual variables (final results are provided in Table II). The overall uncertainty for the measured corrosion rate is about 3%–4%. Furthermore, the experiments show that the corrosion monitoring system can achieve high sensitivity, which is a strong function of the slope of wedge–shaped coating, the dielectric constant and the thickness of the substrate, sensor and coating geometry, and the measurement instrumentation of the system. The experimental results indicate that the sensor is capable of measuring submicrometer thickness changes confidently. Such sensitivity enables specific designs of the sensor to suit the need for different applications and, in particular, for short term, online fireside corrosion monitoring. Further field testing is needed to examine the feasibility of the sensor concept for power plant applications because many environmental parameters cannot be completely simulated in the laboratory, such as ash deposits on the sensor, large temperature gradients within the ash deposits, metal and flue gas temperature fluctuations inside the boilers, and the electrical noise in the environment.

IV. CONCLUSIONS

The laboratory corrosion experiments have demonstrated that the sensor concept and measurement system are capable of short term, online monitoring of metal loss. Several conclusions can be drawn from the current study:

(1) Laboratory proof-of-concept experiments demonstrated the feasibility of the sensor concept and design. The sensor fabricated can perform metal loss measurement at high temperature conditions with a high signal-to-noise ratio and can detect submicrometer thickness changes.
(2) DC magnetron sputtering deposition is a method that can be used to make wedge-shaped coating on ceramic substrates. The coatings survived high temperature environments in our experiment. The fabricated method for the sensors was shown to meet the theoretical design requirements.
(3) The sensor and measurement system obtained the corrosion rate quickly under different temperatures for sputtered low carbon steel in oxidizing conditions. The corrosion rates showed strong dependence on temperature, ranging from 2 nm/h at 200 °C to 2 μm/h at 400 °C. The corrosion followed the Arrhenius rate form and the rate constant were determined based on parameters obtained from the experiments.
(4) Uncertainty analysis indicated that the overall measurement uncertainty was within 4% for the average corrosion rate. The sensitivity of the experimental system indicated that the performance of the sensor and corrosion measurement system could be used for short term, online fireside corrosion monitoring.

Further effort is needed to design and integrate an air-cooled probe with temperature control and a corrosion measurement system for short-term continuous online corrosion monitoring in power plant boilers.

ACKNOWLEDGMENTS

This project is partially funded by Department of Energy (DOE) under Contract No. DE-FG26-01NT41281.

[1] J. N. Harb and E. E. Smith, Prog. Energy Combust. Sci. **16**, 169 (1990).
[2] R. W. Bryers, Prog. Energy Combust. Sci. **22**, 29 (1996).
[3] B. Dooley and P. Chang, Power Plant Chem. **2**, 4 (2000).
[4] A. J. B. Cultler, T. Flatley, and K. A. Hay, J. Combust. **12**, 17 (1980).
[5] R. D. Kane, *Corrosioneering Newsletter* (InterCorr International, Inc., Houston, 2002).
[6] K. Natesan, A. Purohit, and D. L. Rink, Proceedings of the 16th Annual Conference on Fossil Energy Materials, Baltimore, MD, 2002 (unpublished).
[7] K. Natesan and J. H. Park, Int. J. Hydrogen Energy **32**, 3689 (2007).
[8] C. E. Jaske, J. A. Beavers, and N. G. Thompson, Proceedings of the Fourth International Conference on Process Plant Reliability, Houston, TX, 1995, (unpublished).
[9] *ASTM G96–90 Standard Guide for Online Monitoring of Corrosion in Plant Equipment (Electrical and Electrochemical Methods)* (ASTM International, West Conshohocken, 2001).
[10] M. McKenzie and P. R. Vassie, Br. Corros. J., London **20**, 117 (1985).
[11] D. R. Bergstrom, J. Mater. Eng. Perform. **20**, 17 (1981).
[12] V. K. Seth and A. A. Sagues, *Corrosion 83* (NACE, Houston, 1983).
[13] D. C. Crowe and R. A. Yeske, J. Mater. Eng. Perform. **25**, 18 (1986).
[14] D. M. Farrell, W. Y. Mok, and L. W. Pinder, Mater. Sci. Eng., A **120–121**, 651 (1989).
[15] G. Gao, F. H. Stott, J. L. Dawson, and D. M. Farrell, Oxid. Met. **33**, 79 (1990).
[16] K. A. Davis, G. C. Green, T. Linjewile, and S. Harding, Proceedings of the Joint International Combustion Symposium AFRC/JFRC/IEA, Kauai, HI, 2001 (unpublished).
[17] K. Hladky and J. L. Dawson, Corros. Sci. **22**, 231 (1982).
[18] K. Hladky and J. L. Dawson, Corros. Sci. **21**, 317 (1981).
[19] P. R. Roberge, R. Beauudon, and V. S. Sastri, Corros. Sci. **29**, 1231 (1989).
[20] S. Magaino, Corros. Eng. **37**, 629 (1988).